DOI: 10.1002/ejic.200800789

Reaction of (Carbonyl)triruthenium with Acetylferrocene Thiosemicarbazone: Synthesis, X-ray Diffraction, and Insight into the Solution Structures

Jing-Mu Yang,[a,b] Bin Hu,[a] Xiao-Xue Hu,[a] and Chun-Gu Xia*[a]

Keywords: Ruthenium / Carbonyl ligands / Multinuclear compounds / Structure elucidation

Reaction of acetylferrocene thiosemicarbazone [L] with $Ru_3(CO)_{12}$ was investigated. Two new complexes, $Ru_3(CO)_9$-[L-H] (**1**) and $Ru_2(CO)_4[L]_2$ (**2**) were isolated. They were characterized by IR, ^1H NMR, and ^{13}C NMR spectroscopic analysis. The crystal structures of **1** and **2** were also determined. In trinuclear cluster **1**, the acetylferrocene thiosemicarbazone ligand was deprotonated and acted as an N,S-chelating ligand as well as a sulfur bridge. Dinuclear compound **2** is the first bis(cycloruthenated acetylferrocene thiosemicarbazone) carbonyl derivative. This complex contains two ruthenium atoms in a dinuclear structure with a $C_{ferrocene}$, N, S_2, and $(CO)_2$ coordination sphere for each ruthenium atom, as both L ligands act as a $C_{ferrocene}$, N, S_2 chelate, and sulfur bridge. The behavior of **1** and **2** under electrospray ionization mass spectrometry (ESI-MS) was studied and the key intermediate $Ru(CO)_2$[L-H] (**3**) in the formation of **2** was directly detected in the reaction solution.

Introduction

The chemistry of transition-metal carbonyl clusters with organosulfur ligands is being widely developed due to its importance in both bioinorganic chemistry and synthetic chemistry. The chemistry of (carbonyl)triruthenium clusters has proved to be an important entry into the basic understanding of the fundamental processes occurring on carbonyl polymetallic units. Additionally, thiosemicarbazones are an important class of organic ligands, as they can coordinate as neutral ligands or in their deprotonated forms. In mononuclear or dinuclear transition-metal complexes, thiosemicarbazone ligands are known to bind to metal ions as neutral, deprotonated N,S bidentate,[1] or N,S,X (X = N, O, C)-tridentate[2] donors to form five- or four-membered chelate rings. Although a number of studies of the coordination behavior of thiosemicarbazone derivatives have concerned high-oxidation-state transition-metal cations, there is little structural information on low-oxidation-state trinuclear complexes[3] with thiosemicarbazones.

Here we report the investigation of the reaction of (carbonyl)triruthenium with acetylferrocene thiosemicarbazone (η^5-C_5H_5)Fe(η^5-C_5H_4)C(Me)=NN(H)C(S)NH(Me) [L][4] in thf. During this reaction, two products were obtained. Cluster **1** has an unsymmetrical triruthenium triangle framework, in which the ligand is deprotonated and acts as a bidentate N,S donor as well as a sulfur bridge. Dinuclear compound **2** consists of a multiring system with a RuS_2Ru[5] core, and the nondeprotonated ligand is in the unusual cycloruthenated ($C_{ferrocene}$,N,S)-tridentate[6] coordination mode, resulting in a significant increase in the stability of **2**.

Recent developments in electrospray ionization mass spectrometry (ESI-MS)[7] have enabled the investigation of metal carbonyl ions in solution.[8] We used this method to characterize **1** and **2** and directly detect the key intermediate, $Ru(CO)_2$(L-H) (**3**), in the reaction solution.

Results and Discussion

Treatment of a thf solution of $Ru_3(CO)_{12}$ with (η^5-C_5H_5)Fe(η^5-C_5H_4)C(Me)=NN(H)C(S)NH(Me) [L] in a 1:1 ratio at 40 °C for 6 h gave $Ru_3(CO)_9$[L-H] (**1**) and $Ru_2(CO)_4[L]_2$ (**2**) as the major products. The yield of **2** increases with higher reaction temperatures and longer reaction times. For convenience, the compounds and reaction are shown in Scheme 1.

The core of the $Ru_3(CO)_9$[L-H] (**1**) cluster is presented in Figure 1. Selected bond lengths and angles are listed in Table 1. The Ru–Ru bond lengths are Ru1–Ru2 2.8416(7), Ru1–Ru3 2.7883(7), and Ru2–Ru3 2.8134(7) Å. This indicates that the three ruthenium atoms form an unsymmetrical triangle. The Ru1–S1 distance is 0.0579 Å shorter than the Ru2–S1 bond length. The monodeprotoned L binds as an N,S-chelate through N1 and S1 to Ru1 to form a five-membered chelate ring with a bite angle of 80.56° (which

[a] State Key Laboratory for Oxo Synthesis and Selective Oxidation, Lanzhou Institute of Chemical Physics, Chinese Academy of Sciences,
Lanzhou 730000, P. R. China
Fax: +86-931-4968129
E-mail: cgxia@lzb.ac.cn
[b] Graduate School of Chinese Academy of Sciences, Beijing, 100039, P. R. China

Supporting information for this article is available on the WWW under http://www.eurjic.org or from the author.

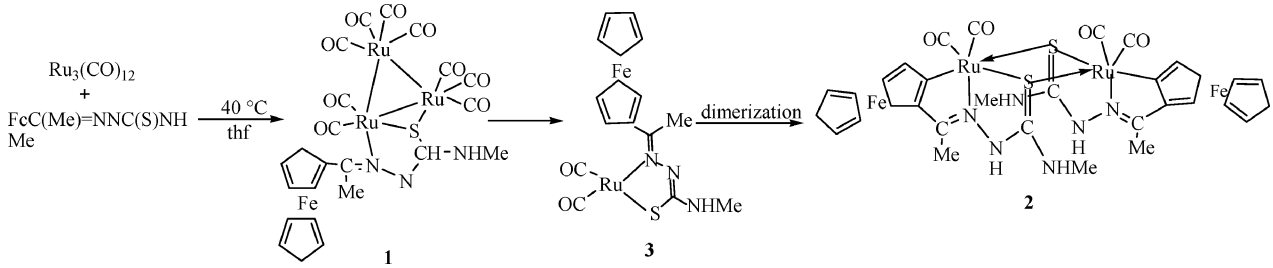

Scheme 1. An overview of the reaction of L with $Ru_3(CO)_{12}$.

closely resembles that in the single metal ion compound[9]) as well as edge-bridging (through μ_2-S1 to Ru1 and Ru2). The two C–N distances, C6–N1 and C8–N2, are 1.293(7) and 1.295(7) Å, respectively, which indicates that the coordinated L has greater conjugation and more delocalized electron density than the uncoordinated L. All nine CO ligands are in distinguishable sites. The room-temperature ^{13}C NMR spectroscopic data are consistent with the molecular structure found in the crystal persisting in solution.

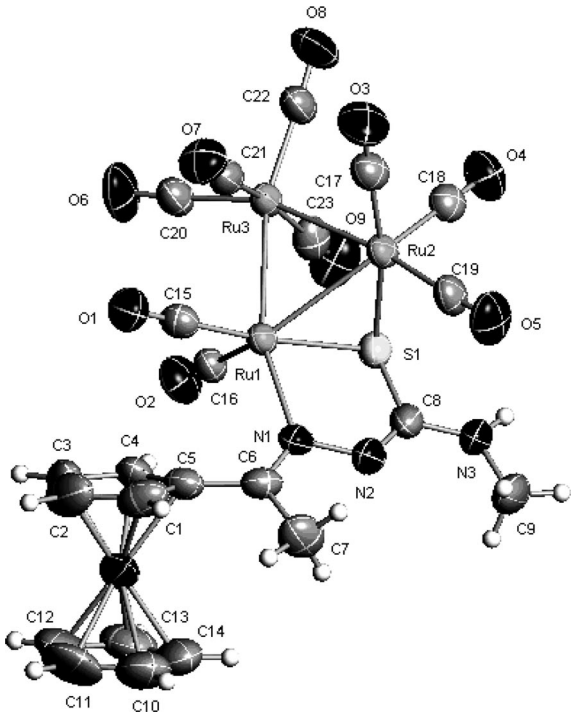

Figure 1. The molecular structure of **1**.

The dinuclear compound $Ru_2(CO)_4[L]_2$ (**2**, Figure 2; selected bond lengths and angles are listed in Table 2) is the first example in which L acts as a cycloruthenated ($C_{ferrocene}$,N,S)-tridentate ligand without deprotonation. The ligand coordinates through the imine nitrogen, sulfur, and carbon atoms of the substituted Cp ring to form two five-membered chelate rings to one ruthenium atom, with the *ortho* H atom of the cyclopentadienyl ring having been displaced in the cyclometalation reaction. The molecule lies on a crystallographic twofold axis, which passes through the center of the four-membered ring of the two Ru atoms and the two bridging S atoms. The two symmetry-related

Table 1. Selected bond lengths and angles for **1**.

Bond lengths [Å]			
Ru1–Ru2	2.8416(7)	Ru2–S1	2.4025(15)
Ru1–Ru3	2.7883(7)	N1–C6	1.293(7)
Ru2–Ru3	2.8134(7)	N2–C8	1.295(7)
Ru1–N1	2.190(4)	N1–N2	1.397(6)
Ru1–S1	2.3446(14)	S1–C8	1.771(6)
Bond angles [°]			
C16–Ru1–N1	104.3(2)	C15–Ru1–N1	100.3(2)
C16–Ru1–S1	96.13(18)	C15–Ru1–S1	171.08(18)
N1–Ru1–S1	80.56(12)	C16–Ru1–Ru3	89.14(17)
C15–Ru1–Ru3	92.54(17)	N1–Ru1–Ru3	160.87(11)
S1–Ru1–Ru3	84.56(4)	N1–Ru1–Ru2	101.29(11)
S1–Ru1–Ru2	54.17(4)	Ru3–Ru1–Ru2	59.954(15)

Ru atoms are in a distorted octahedral coordination environment, with two bridging S atoms in the equatorial plane and two bridging Ru–S distances of 2.514(2) and 2.451(2) Å. These distances are longer than those observed in **1**. The C13–N3 [1.311(9) Å] bond length becomes longer, increasing its single-bond character. The N–Ru–S bite angle of **2** [N3–Ru–S 79.47(18)°] is only slightly smaller than that of **1**.

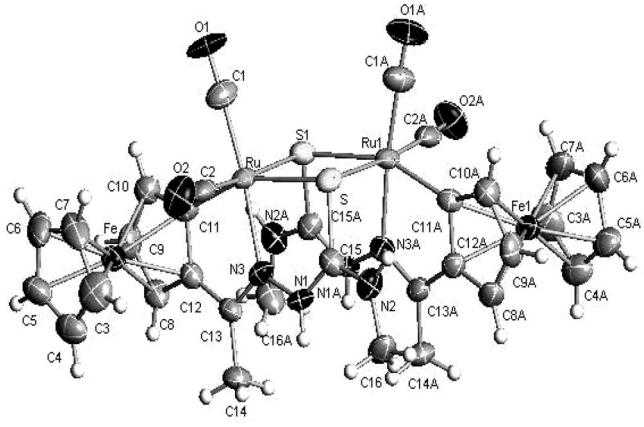

Figure 2. The molecular structure of **2**.

In the NH-stretching region (3400–3090 cm^{-1}) of the IR spectrum, it is clear that deprotonation makes the spectrum of **1** (3412 cm^{-1}) different from that of **2** (3439, 3091 cm^{-1}). The presence of absorption bands at 829 and 816–804 cm^{-1} are assigned to the ν(C=S) band in the IR spectra of **1** and **2**, respectively. The medium intensity bands around 1585 and 1547–1573 cm^{-1} in the spectra of **1** and **2** are assigned

Table 2. Selected bond lengths and angles for **2**.

Bond lengths [Å]			
Ru–N3	2.105(6)	N1–C15	1.292(9)
Ru–S	2.451(2)	N3–C13	1.311(9)
Ru–S#1	2.514(2)	N1–N3	1.385(8)
S–C15	1.788(8)		
Bond angles [°]			
C2–Ru–N3	89.5(3)	N3–Ru–S	79.47(18)
C1–Ru–N3	174.0(3)	C2–Ru–S#1	175.4(2)
C11–Ru–N3	78.8(3)	C1–Ru–S#1	86.9(3)
C2–Ru–S	94.5(3)	C11–Ru–S#1	89.0(2)
C1–Ru–S	106.5(3)	N3–Ru–S#1	94.18(18)
C11–Ru–S	156.4(2)	S–Ru–S#1	83.54(8)

to ν(C=N), indicating that C=N groups are involved in coordination. In the carbonyl region, there are four carbonyl stretching bands at 2089, 2049, 2002, and 1934 cm^{-1} that appear in the spectrum of **1**. The IR spectrum of **2** shows two strong bands at 2027 and 1958 cm^{-1}.

The ^1H and ^{13}C NMR results for **1** were obtained in $CDCl_3$ solution. Due to the configuration and the π-electron delocalization of **1**, the four nuclei of the substituted Cp rings have different chemical shifts, and each nuclear signal is split by coupling with all of the other nuclei. Thus, each nucleus gives the multiplet pattern shown at δ = 4.59, 4.61, 4.65, and 5.03 ppm. There is an upfield shift of the NH signal to δ = 4.92 ppm. The room-temperature ^{13}C NMR spectrum of **1** shows all but one of the nine resonances in the carbonyl region at δ = 185.66, 190.45, 193.42, 197.49, 199.00, 203.74, 204.64, and 204.86 ppm (there is an accidental coincidence of two carbonyl signals at room temperature).

In **2**, the delocalization of electron density in the multiring system gives rise to a ring current. Because of the ring-current effect, a pronounced tendency towards line broadening was observed for **2** in the nonpolar solvent $CDCl_3$. The ^1H NMR spectrum of **2** in [D_6]acetone showed that the ring current shields the NH protons and induces large upfield shifts, and as a consequence, the chemical shifts of the two NH protons appear at δ = 2.57 and 2.82 ppm, respectively. There are three peaks corresponding to the substituted Cp ring at δ = 3.76, 4.39, and 4.72 ppm. In the ^{13}C NMR spectrum of **2**, the broad, low-intensity metalated carbon signal at δ = 103.49 ppm was observed due to the nuclear Overhauser effect.[10] These data provided evidence of cycloruthenation of the substituted Cp ring. The chemical shifts of the carbonyl ligands in the ^{13}C NMR spectrum show two signals at δ = 194.03 and 201.49 ppm as a result of the high rigidity and symmetry of the molecular structure.

Although single-crystal structure analyses of the products can provide important insight into mechanistic details, the direct detection of short-lived intermediates of the reaction in solution by ESI-MS methods can detail the reaction mechanism in a stepwise fashion. The use of formic acid/methanol as the mobile phase in ESI-MS allows this technique to be used to analyze the novel species of this reaction.

First, the ESI-MS technique was employed to examine the pure compounds (Figure 3). The skimmer cone voltage was maintained at a low value (5 V) to minimize the fragmentation of ions. The ESI-MS (positive mode) analysis of pure trinuclear cluster **1** (*m*/*z* = 869) and dinuclear product **2** (*m*/*z* = 942) in methanol containing formic acid showed the presence of the molecular peaks corresponding to the intact parent ions after electron capture. However, the loss of a number of CO ligands is only observed in the ESI mass spectrum of **1**, and even at higher cone voltages, the loss of CO is especially difficult with **2**.

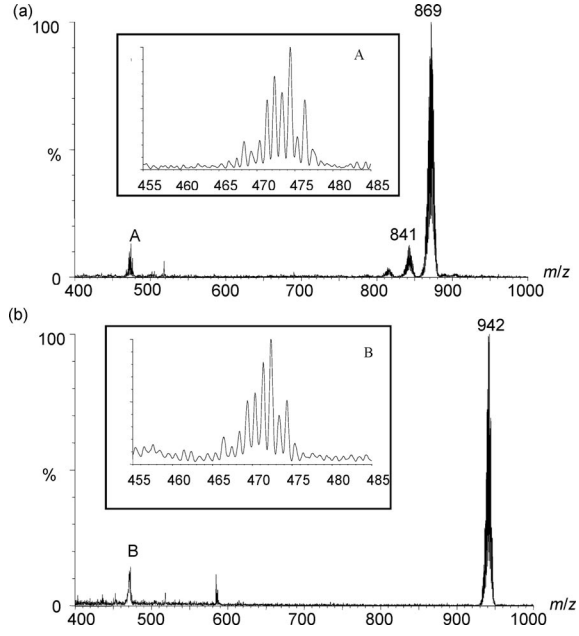

Figure 3. ESI spectrum of a MeOH solution of (a) **1** and (b) **2**.

The reaction of $Ru_3(CO)_{12}$ with acetylferrocene thiosemicarbazone in thf at 40 °C was also monitored by positive-ion ESI-MS analysis. As shown in Figure 4, after heating the reaction system for 30 min, peaks are observed at *m*/*z* = 785 and 813, values typical for carbonyl loss from $Ru_3(CO)_9$[L-H] and corresponding to the ions $Ru_3(CO)_6$[L-H] and $Ru_3(CO)_7$[L-H], respectively. A peak corresponding to dinuclear compound $Ru_2(CO)_4[L]_2$ is also observed at *m*/*z* = 942. In the range of *m*/*z* = 590–640, two peaks, which may be assigned to the triruthenium cluster ions $Ru_3(CO)_{11}(H_3O)$ and $Ru_3(CO)_9(H_3O)_2$, are observed at *m*/*z* = 630 and 595, respectively. These ions are derived from $Ru_3(CO)_{12}$.

It is noteworthy that all three ESI mass spectra of the reaction mixture contain peaks in the mass range between *m*/*z* = 465 and 480 (A, B, C, Figures 3 and 4). To obtain more information for justifying the peak assignments above, we compared the experimental isotopic patterns of A, B, and C (see insets). All three observed isotope patterns of the molecular ion peaks contain the highly characteristic isotope pattern for ruthenium.[11] Peak centroid A is observed at *m*/*z* = 474 and may be readily assigned to the $Ru(CO)_2$[L-H] + 3H ion derived directly from the fragmentation of **1**. Peak B at *m*/*z* = 472 may be assigned to the

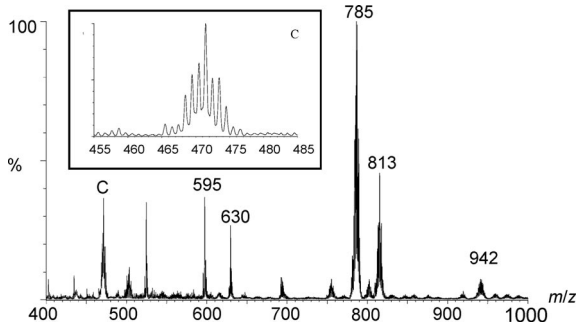

Figure 4. ESI spectrum of the reaction solution.

ion $Ru(CO)_2L$, derived from the fragmentation of **2**. The observed peak C at m/z = 471 in Figure 4 confirms the existence of intermediate $Ru(CO)_2$[L-H] (**3**) and could originate either from the preexistence of **3** ions in the sample solution or by the fragmentation of products **1** under the electrospray conditions.

Conclusions

These results, taken in conjunction with the well-established structural features of the two products, allow us to rationalize the sequence of reactions as summarized in Scheme 1: Initial substitution of CO ligands by L to form cluster $Ru_3(CO)_9$[L-H] (**1**), in which deprotonation of the ligand takes place. Next, the breakdown of **1** gives rise to intermediate $Ru(CO)_2$[L-H] (**3**). The activation of the chelated Ru atom and S atom must occur along the cleavage of one S–Ru bond and two Ru–Ru bonds, and this should make cycloruthenation of the ferrocenyl group easy. Finally, the dimerization of **3** occurs rapidly to generate **2**.

Experimental Section

General Remarks: All reactions were carried out in redistilled solvents under a nitrogen atmosphere by using standard Schlenk techniques. $Ru_3(CO)_{12}$ was from our laboratory, and acetylferrocene thiosemicarbazone was prepared by using a literature procedure.[4a] Column chromatography was carried out by using silica gel columns of 160–200 mesh. The purified products were divided into two parts, one portion was kept in a vacuum dryer as the sample for NMR spectroscopy, elemental analyses, and IR study; the other portion was recrystallized from hexane/CH_2Cl_2 at –20 °C for X-ray diffraction analysis. The existence of dichloromethane molecules in the crystal lattice occurred during recrystallization. Infrared spectra were recorded with a Nicolet 405 FTIR spectrometer, and NMR spectra were obtained with a Bruker AC 400 NMR spectrometer operating at 400 MHz for ^{1}H NMR and 100 MHz for ^{13}C NMR spectroscopy. The ^{1}H and ^{13}C NMR chemical shifts are reported relative to TMS. Elemental analyses (C, H) were performed with a Perkin–Elmer 2400-type analyzer. The structures of products **1** and **2** were determined by single-crystal X-ray diffraction. Suitable crystals were mounted on the tips of glass fibers with perfluoropolyether oil coated on them. Data were collected at 293 K with a Respecton, an R-AXIS-IV diffractometer (Mo-K_α radiation) equipped with an imaging plate area detector and a rotating anode. The structure was solved by direct methods (SHELXS-97) and expanded by using Fourier techniques. All non-hydrogen atoms were refined anisotropically by full-matrix least-squares on F2 by using the SHELXL-97 crystallographic program package. Electrospray mass spectra were recorded with a Waters ZQ4000 ESI-MS spectrometer operating in positive-ion mode. The mobile phase was formic acid/methanol. For monitoring reactions, ca. 0.5-mL samples of the mixture were extracted by syringe, diluted under an atmosphere of argon with methanol, and injected into the spectrometer by a syringe pump. The source temperature was 100 °C, and nitrogen was used as both the nebulizing and drying gas. The skimmer cone voltage was maintained at a low value (5 V) to minimize the fragmentation of ions.

Reaction of $Ru_3(CO)_{12}$ with FcC(Me)=NNC(S)NHMe: A 250-mL three-necked flask with a condenser and a gas inlet was charged with $Ru_3(CO)_{12}$ (200 mg, 0.313 mmol), FcC(Me)=NNC(S)NHMe (93.9 mg, 0.313 mmol), and thf (40 mL). The reaction mixture was heated at 40 °C for 6 h under a slow nitrogen sweep, during which time the solution changed from saffron yellow to chrysoidine. The solvent was removed under reduced pressure, and the residual solid was purified by column chromatography (silica gel; petroleum 60–90/CH_2Cl_2, 6:1). The second orange band, which included **1** (26 mg, 9.56%), and a third red band, which included **2** (66 mg, 22.39%), were collected, and the solvent was removed under reduced pressure. Crystals suitable for X-ray diffraction analysis were obtained by recrystallization from hexane/CH_2Cl_2 at –20 °C.

1: FTIR (KBr): $\tilde{\nu}$ = 2089 (s), 2049 (s), 2002 (vs), 1934 (m) [ν(CO)], 1585 (m) [ν(C=N)] cm^{-1}. ^{1}H NMR (400 MHz, $CDCl_3$): δ = 2.56 (s, 3 H, CH_3), 2.92 (d, 3 H, CH_3), 4.24 (s, 5 H, C_5H_5), 4.59 (sext., 1 H, C_5H_4), 4.61 (sext., 1 H, C_5H_4), 4.65 (quint., 1 H, C_5H_4), 4.92 (d, 1 H, NH), 5.03 (quint, 1 H, C_5H_4) ppm. ^{13}C NMR (100 MHz, $CDCl_3$): δ = 26.77, 32.30, 69.30, 69.72, 69.89, 71.15, 73.26, 88.20, 172.31, 172.94, 185.66, 190.43, 193.40, 197.49, 198.99, 203.72, 204.64, 204.86 ppm. $C_{23}H_{16}FeN_3O_9Ru_3S$(869.43): calcd. C 28.93, H 1.68; found C 28.89, H 1.70.

2: FTIR (KBr): $\tilde{\nu}$ = 2027 (vs), 1958 (vs) [ν(CO)], 1573 (m), 1546 (m) [ν(C=N)] cm^{-1}. ^{1}H NMR (400 MHz, [D$_6$]acetone): δ = 2.57 (s, 1 H, NH), 2.61 (d, 3 H, CH_3), 2.79 (t, 3 H, CH_3), 2.82 (s, 1 H, NH), 3.76 (s, 1 H, C_5H_3), 4.13 (s, 5 H, C_5H_5), 4.39 (s, 1 H, C_5H_3), 4.72 (s, 1 H, C_5H_3) ppm. ^{13}C NMR (100 MHz, $CDCl_3$): δ = 15.70, 32.56, 64.94, 69.76, 70.10, 76.02, 93.61, 103.43, 163.07, 170.50, 194.03, 201.49 ppm. $C_{32}H_{32}Fe_2N_6O_4Ru_2S_2$ (942.52): calcd. C 40.72, H 3.39; found C 40.76, H 3.43.

X-ray Crystallography

1: $C_{23}H_{16}FeN_3O_9Ru_3S$, M_r = 869.43, monoclinic, space group $P2_1/c$, a = 9.2352(12) Å, b = 22.731(3) Å, c = 15.622(2) Å, α = 90°, β = 106.133(2)°, γ = 90°, V = 3150.4(7) Å^3, Z = 4, ρ = 2.012 g cm^{-3}, F(000) = 1852, crystal size 0.490 × 0.345 × 0.220 mm^3, R_1 = 0.0446 [wR_2 = 0.0968, $I > 2\sigma(I)$], R_1 = 0.0689 (wR_2 = 0.1026, all data), GOF = 0.858. Data/restraints/parameters of 6790/3/394, T = 293(2) K, λ = 0.71073 Å.

2: $C_{32}H_{32}N_6O_4S_2Fe_2Ru_2$, M_r = 942.52, monoclinic, space group $P2/n$, a = 7.8664(12) Å, b = 10.7140(16) Å, c = 22.582(3) Å, α = 90°, β = 99.569(3)°, γ = 90°, V = 1876.7(5) Å^3, Z = 2, ρ = 1.818 g cm^{-3}, F(000) = 1024, crystal size 0.396 × 0.192 × 0.047 mm^3, R_1 = 0.0657 [wR_2 = 0.1371, $I > 2\sigma(I)$], R_1 = 0.1262 (wR_2 = 0.1576, all data), GOF = 0.854. Data/restraints/parameters of 4307/0/233, T = 293(2) K, λ = 0.71073 Å.

CCDC-648043 (for **1**) and -242282 (for **2**) contain the supplementary crystallographic data for this paper. These data can be obtained free of charge from The Cambridge Crystallographic Data Centre via www.ccdc.cam.ac.uk/data_request/cif.

Supporting Information (see footnote on the first page of this article): ^{1}H NMR, ^{13}C NMR, and IR spectra for compounds **1** and **2**.

Acknowledgments

The authors acknowledge the support of this work by the National Science Fund for Distinguished Young Scholars of China (No. 20625308).

[1] a) G. P. Gabian, E. M. V. Lopez, H. Braband, U. Abram, *Inorg. Chem.* **2005**, *44*, 834–836; b) I. G. Santos, U. Abram, R. Alberto, E. V. Lopez, A. Sanchez, *Inorg. Chem.* **2004**, *43*, 1834–1836; c) F. Basuli, M. Ruf, C. G. Pierpont, S. Bhattacharya, *Inorg. Chem.* **1998**, *37*, 6113–6116; d) E. L. Torres, M. A. Mendiola, C. J. Pastor, *Inorg. Chem.* **2006**, *45*, 3103–3112.

[2] a) J. G. Tojal, L. Lezama, J. L. Pizarro, M. Insausti, M. I. Arriortua, T. Rojo, *Polyhedron* **1999**, *18*, 3703–3711; b) U. Abram, K. Ortner, R. Gust, K. Sommer, *J. Chem. Soc., Dalton Trans.* **2000**, 735–744; c) M. Carcelli, A. Fochi, P. Pelagatti, G. Pelizzi, U. Russo, *J. Organomet. Chem.* **2001**, *626*, 161–167.

[3] V. P. Kirin, V. A. Maksakov, A. V. Virovets, S. A. Popov, A. V. Tkachev, *J. Organomet. Chem.* **2004**, *689*, 2535–2542.

[4] a) A. A. El-Asmy, Y. M. Shaibi, I. M. Shedaiwa, M. A. Khattab, *Synth. React. Inorg. Met.-Org. Chem.* **1990**, *20*, 461–481; b) J. S. Casas, M. V. Castaño, M. C. Cifuentes, A. Sánchez, J. Sordo, *Polyhedron* **2002**, *21*, 1651–1660.

[5] a) H. Uemura, M. Kawano, T. Watanabe, T. Matsumoto, K. Matsumoto, *Inorg. Chem.* **1992**, *31*, 5137–5139; b) C. A. Toledano, E. Delgado, B. Donnadieu, *Eur. J. Inorg. Chem.* **2003**, 562–568; c) A. Amoedo, L. A. Adrio, J. M. Antelo, J. Martínez, M. T. Pereira, A. Fernández, J. M. Vila, *Eur. J. Inorg. Chem.* **2006**, 3016–3021.

[6] J. M. Vila, E. Gayoso, M. T. Pereira, *Eur. J. Inorg. Chem.* **2004**, 2937–2942.

[7] a) J. C. Traeger, *Int. J. Mass Spectrom.* **2000**, *200*, 387–401; b) P. J. Dyson, A. K. Hearley, B. F. G. Johnson, P. R. R. Langridge-Smith, J. S. McIndoe, *Inorg. Chem.* **2004**, *43*, 4962–4973.

[8] a) C. Evans, K. M. Mackay, B. K. Nicholson, *J. Chem. Soc., Dalton Trans.* **2001**, 1645–1649; b) P. J. Dyson, A. K. Hearley, B. F. G. Johnson, *Organometallics* **2001**, *20*, 3970–3974; c) G. Critchley, P. J. Dyson, B. F. G. Johnson, J. S. McIndoe, *Organometallics* **1999**, *18*, 4090–4097; d) W. Henderson, J. S. McIndoe, B. K. Nicholson, P. J. Dyson, *Chem. Commun.* **1996**, 1183–1184.

[9] F. Basuli, S. M. Peng, S. Bhattacharya, *Inorg. Chem.* **2000**, *39*, 1120–1127.

[10] C. López, R. Bosque, X. Solans, M. Font-Bardia, J. Silver, G. Fern, *J. Chem. Soc., Dalton Trans.* **1995**, 1839–1849.

[11] a) V. W. Yam, C. Ko, B. W. Chu, N. Zhu, *Dalton Trans.* **2003**, 3914–3921; b) J. M. Slocik, K. V. Somayajula, R. E. Shepherd, *Inorg. Chim. Acta* **2001**, *320*, 148–158; c) J. A. Kenny, K. Versluis, A. J. R. Heck, T. Walsgrovec, M. Wills, *Chem. Commun.* **2000**, 99–100; d) P. J. Dyson, A. K. Hearley, B. F. G. Johnson, T. Khimyak, J. S. McIndoe, P. R. R. Langridge-Smith, *Organometallics* **2001**, *20*, 3970–3974.

Received: August 7, 2008
Published Online: November 10, 2008

